Fungal Genetics and Biology 167 (2023) 103800

Contents lists available at ScienceDirect

Fungal Genetics and Biology

journal homepage: www.elsevier.com/locate/yfgbi

Detection and quantification of the histone code in the fungal genus *Aspergillus*

Xin Zhang [a,b], Roberta Noberini [c], Alessandro Vai [c], Tiziana Bonaldi [c,d,*,1], Michael F. Seidl [a,*,1], Jérôme Collemare [b,*,1]

[a] Theoretical Biology & Bioinformatics Group, Department of Biology, Utrecht University, Padualaan 8, 3584 CH Utrecht, The Netherlands
[b] Westerdijk Fungal Biodiversity Institute, Uppsalalaan 8, 3584 CT Utrecht, The Netherlands
[c] Department of Experimental Oncology, European Institute of Oncology (IEO) IRCCS, Via Adamello 16, 20139 Milan, Italy
[d] Department of Oncology and Haematology-Oncology, University of Milano, Via Santa Sofia 9/1, 20122 Milano, Italy

ARTICLE INFO

Keywords:
Histone methylation
Histone acetylation
Histone extraction
Mass spectrometry
Aspergillus niger
Aspergillus nidulans
Aspergillus fumigatus

ABSTRACT

In eukaryotes, the combination of different histone post-translational modifications (PTMs) – the histone code – impacts the chromatin organization as compact and transcriptionally silent heterochromatin or accessible and transcriptionally active euchromatin. Although specific histone PTMs have been studied in fungi, an overview of histone PTMs and their relative abundance is still lacking. Here, we used mass spectrometry to detect and quantify histone PTMs in three fungal species belonging to three distinct taxonomic sections of the genus *Aspergillus* (*Aspergillus niger*, *Aspergillus nidulans* (two strains), and *Aspergillus fumigatus*). We overall detected 23 different histone PTMs, including a majority of lysine methylations and acetylations, and 23 co-occurrence patterns of multiple histone PTMs. Among those, we report for the first time the detection of H3K79me1, H3K79me2, and H4K31ac in Aspergilli. Although all three species harbour the same PTMs, we found significant differences in the relative abundance of H3K9me1/2/3, H3K14ac, H3K36me1 and H3K79me1, as well as the co-occurrence of acetylation on both K18 and K23 of histone H3 in a strain-specific manner. Our results provide novel insights about the underexplored complexity of the histone code in filamentous fungi, and its functional implications on genome architecture and gene regulation.

1. Introduction

In eukaryotes, the genetic information is stored within the nucleus as chromatin, a complex of DNA and proteins of which the basic unit is the nucleosome (Luger et al., 1997). A nucleosome is composed of a histone octamer formed by two copies of each histone protein H2A, H2B, H3, and H4 wrapped by a DNA stretch of 145–147 bp (Luger et al., 1997). Nucleosomes are linked by 30–50 bp DNA sequence and the linker histone protein H1 (Luger et al., 1997). Histone proteins are highly conserved, consistent with their fundamental roles in structuring, scaffolding, and packaging DNA (van Holde, 1989). Each histone protein contains a globular central domain that interacts with the nucleosomal DNA, and a lysine- and arginine-rich N-terminal tail that is subject to a diverse array of chemical modifications (van Holde, 1989). These histone post-translational modifications (PTMs) contribute to the regulation of chromatin accessibility by two mechanisms: first, they directly alter chromatin packaging by changing histone proteins' net charges; second, histone PTM-specific binding proteins are recruited and can influence inter-nucleosomal interactions (Henikoff and Shilatifard, 2011). The resulting chromatin changes lead to transitions between inaccessible and transcriptionally silent chromatin regions, the so-called (facultative or constitutive) heterochromatin, and the accessible and transcriptionally active regions, the so-called euchromatin (Henikoff and Shilatifard, 2011). The combination of different histone PTMs at a single genomic locus – the histone code – contributes to the accessibility of chromatin for the transcriptional machinery, thereby regulating gene expression to influence not only growth and development but also responses to environmental challenges (van Holde, 1989).

In the last decades, a plethora of different histone PTMs have been uncovered in diverse organisms from plants to human, with an enrichment of histone mono-, di-, and tri-methylation (me) and acetylation (ac) (Huang et al., 2015). Accordingly, the vast majority of studies in

* Corresponding authors.
E-mail addresses: tiziana.bonaldi@ieo.it (T. Bonaldi), m.f.seidl@uu.nl (M.F. Seidl), j.collemare@wi.knaw.nl (J. Collemare).
[1] These authors contributed equally.

https://doi.org/10.1016/j.fgb.2023.103800
Received 31 January 2023; Received in revised form 30 March 2023; Accepted 24 April 2023
Available online 3 May 2023

fungi thus far have focused on these PTMs (Collemare and Seidl, 2019). Euchromatin has been typically associated with methylations on histone protein H3 at lysine 4 (K4), K36 and K79, and acetylations on H3 at K9, K14, K18, K23, and K27 and H4 at K5, K8, K12, and K16 (Shilatifard, 2006; Bhaumik et al., 2007). For instance, in the budding yeast *Saccharomyces cerevisiae* methylation on the lysine 4 of histone protein H3 (H3K4me) and H3K36me are enriched at the 5′ and 3′ end of actively transcribed genes, respectively, while H3K79me has been detected at the coding regions of active genes (Farooq et al., 2016; Pokholok et al., 2005). H3K4ac locates just upstream of actively transcribed genes (Guillemette et al., 2011), and H3K9ac and H4K5ac have been shown to induce transcription elongation *in vitro* (Gates et al., 2017). In members of the filamentous Aspergilli, some of these euchromatin marks are shown to positively influence the production of secondary metabolites (SMs), including H3K4me in *Aspergillus oryzae* (Shinohara et al., 2016); H3K36me, H3K14/18/23ac (acetylation on either of these lysines), and H4K16ac in *Aspergillus flavus* (Chen et al., 2022; Zhuang et al., 2022); H3K9ac in *Aspergillus fumigatus* (Zhang et al., 2021) and *Aspergillus nidulans* (Reyes-Dominguez et al., 2010); and H3K27ac in *A. fumigatus* (Adlakha et al., 2016). Especially, the diverse functions of histone acetyltransferase complex (SAGA complex) or its crucial subunits (Gcn5 and AdaB) have been extensively studied in *A. nidulans*, in which they can influence asexual development (Cánovas et al., 2014), production of natural products in response to the interaction with bacteria (Nützmann et al., 2011), and nucleosome positioning (Reyes-Dominguez et al., 2008). Histone PTMs can also be linked to gene silencing, as first shown for H3K9me and H3K27me that are marks for constitutive heterochromatin in animals and plants (Henikoff and Shilatifard, 2011). H3K9me3 plays a similar role in fungi as this PTM is typically located at telomeres, sub-telomeres, centromeres, and transposon-rich regions in the fission yeast *Schizosaccharomyces pombe* (Yamada et al., 2005), the filamentous model fungus *Neurospora crassa* (Rountree and Selker, 2010) and many other filamentous fungi (Freitag, 2017). H3K9me can influence SM biosynthesis in *A. nidulans* (Reyes-Dominguez et al., 2010) and *A. fumigatus* (Colabardini et al., 2022), however, as H3K9me is not always found located near SM gene clusters, it remains obscure whether it is directly linked to the regulation of SM gene clusters in Aspergilli and raises the possibility of the interaction of multiple histone PTMs or the distal regulation based on a higher level of chromatin structure. Facultative heterochromatin is linked with H3K27me3, and unsurprisingly, it does generally not overlap with the euchromatin mark H3K4me in the cereal pathogens *Fusarium graminearum* (Connolly et al., 2013) and *Fusarium fujikuroi* (Wiemann et al., 2013). By contrast, SET7 (KMT6) that is responsible for H3K27me is absent in Aspergilli, and consequently, no H3K27me is detected (Zhang et al., 2022). Although many PTMs have been clearly associated with gene activation or repression only, their effect can also be more subtle, depending on the genomic context. In *N. crassa* and *F. fujikuroi*, H3K36me catalyzed by SET-2 drives gene expression at the euchromatic region, while H3K36me catalyzed by ASH-1 at sub-telomeric regions is associated with gene repression (Bicocca et al., 2018; Janevska et al., 2018). This complexity is even higher when considering the role of less abundant histone PTMs like histone acylation, phosphorylation, ubiquitination, and sumoylation, which thus far have been mostly reported in human (Tan et al., 2011). In fungi, such less abundant PTMs have been only reported scarcely in *S. cerevisiae* (diverse acylations, phosphorylation, ubiquitination, and sumoylation) and *A. nidulans* (phosphorylation, ubiquitination, and sumoylation), and the phosphorylation of histone H3 serine 10 correlates with chromosome condensation (De Souza et al., 2000).

Large-scale mass spectrometry (MS) studies have been performed on bulk histones from model species such as human, yeast, and Arabidopsis to uncover the full pattern of histone PTMs and their interactions (Johnson et al., 2004; Grau-Bové et al., 2022). However, studies in filamentous fungi have mostly focused on quantitative changes of targeted histone PTMs in mutant strains deficient in specific histone-modifying enzymes (Gacek-Matthews et al., 2016; Gacek-Matthews et al., 2015). For instance, mutants of histone H3 demethylase *KdmA* or *KdmB* in *A. nidulans* show increased H3K36me3 or H3K4me3, respectively (Gacek-Matthews et al., 2016; Gacek-Matthews et al., 2015). Our previous evolutionary analysis of 16 chromatin modifier complexes across the *Aspergillus* genus demonstrated the conservation of most of the catalytic genes responsible for a variety of histone PTMs (Zhang et al., 2022). However, we still lack an overview of (co-)occurrence of histone PTMs in filamentous fungi, as well as a better understanding of the quantitative diversity of histone PTMs between different species. Here, we used quantitative MS to uncover histone PTMs in three *Aspergillus* species (*Aspergillus niger*, *A. nidulans*, and *A. fumigatus)* from distinct taxonomic sections and to report their estimated quantitative intra- and inter-species difference.

2. Materials and methods

2.1. Fungal strains and culture

A. niger (wild type strain: NRRL3, CBS 120.49) and *A. fumigatus* (wild type strain: Af293, CBS 126847) were grown on MEA (Malt Extract Agar; Malt Extract Agar Oxoid 50 g/L) medium at 30 °C and 25 °C, respectively, while *A. nidulans* (strains: Wtpaba (genotype: pabaA1) and TN02A25 (genotype: pyrG89 argB2 pabaB22 nku::argB riboB2), kindly provided by Prof. Joseph Strauss) was grown on YAG (Yeast Agar Glucose; 5 g/L yeast extract, 15 g/L agar, 20 g/L D-glucose, 1 mL/L trace elements (Solution A: dissolve 10 g EDTA and 1 g $FeSO_4{\cdot}7H_2O$ in 80 mL water and adjust pH to 5.5; solution B: dissolve 4.4 g $ZnSO_4{\cdot}7H_2O$, 1 g $MnCl_2{\cdot}4H_2O$, 0.32 g $CuSO_4{\cdot}6H_2O$, and 0.22 g $(NH_4)_6Mo_7O_{24}{\cdot}4H_2O$ in 80 mL water; combine solutions A and B, adjust pH to 6.5) medium at 37 °C.

Fungal spores of the four Aspergilli strains were harvested from 4- or 5-day-old sporulating plates with a spreader in 12.5 mL ice-cold ACES (1.822 g/L N-(2-Acetamido)-2-aminoethanesulfonic acid, 0.2 mL/L Tween 80) buffer at the same time. The spore suspension was centrifuged at 2,500 xg at 4 °C for 5 min. The supernatant was discarded, and spores were resuspended in 25 mL ice-cold ACES buffer. The spore suspension was centrifuged at 2,500 xg at 4 °C for 5 min, and the supernatant was discarded. Spores were resuspended in 10 mL ice-cold ACES buffer, and spore concentration was determined with a hemocytometer (Marienfeld, 0.0025 mm^2) or spore counter, and adjusted to 10^7 spores/ mL. For the overnight culturing, 10^7 to 10^8 spores were inoculated in 50 mL liquid medium in a 250 mL flask and incubated at the same temperature as plate culture, 200 rpm, for 16 h. Mycelium were centrifugated at 4,000 xg for 10 min and the supernatant was discarded. The mycelium pellet was washed with 25 mL 0.8 M NaCl, followed by centrifugation at 4,000 xg for 10 min to collect them for histone protein extraction. No obvious difference in regard to growth was observed.

2.2. Histone protein extraction

Histone proteins were extracted according to an adapted histone protein extraction protocol (Zhang et al., 2021). Briefly, the fungal material was freeze-dried, ground with a mortar and pestle, and further disrupted by TissueLyser II (QIAGEN, C.0659). 100 mg ground sample was first resuspended in 1 mL lysis buffer (1 × PBS, 0.5 mM PMSF, 5 μM Leupeptin, 5 μM Aprotinin, and 5 mM Na-butyrate) with high (10%) Triton X-100 concentration and incubated on an orbital shaker at 4 °C for half an hour. Then 10 mL lysis buffer with low (1%) Triton X-100 concentration was added and the sample was incubated for another half an hour. The samples were subsequently sonicated for 30 s with 10 repeats and 30-second break in between each repeat. The crude histone proteins were dissolved in 0.4 N H_2SO_4 and then precipitated in four volumes of acetone. Protein concentration was measured with the Bradford Protein Assay (He, 2011).

2.3. LC-MS/MS analysis of histone PTMs

Samples were separated on a 17% SDS-PAGE gel and histone bands were excised and in-gel digested using a double derivatization protocol that involves propionylation of lysines and N-terminal derivatization with phenyl isocyanate (Noberini et al., 2021). Chemical propionylation of lysines (which occurs on unmodified or mono-methylated residues) impairs trypsin cleavage, resulting in proteolytic cleavage at arginine residues only and the generation of histone peptides of proper length for MS analysis. Peptide mixtures were separated by reversed-phase liquid chromatography and analyzed by MS on an Orbitrap instrument, as previously described (Zhang et al., 2022).

The acquired RAW data were analyzed using the integrated MaxQuant software v.1.6.10. The Uniprot UP000000560, UP000006706, and UP000002530 databases were used for the identification of *A. nidulans, A. niger,* and *A. fumigatus* histone peptides, respectively. Enzyme specificity was set to Arg-C. The estimated false discovery rate was set at a maximum of 1% at both peptide and protein levels. The mass tolerance was set to 4.5 ppm for precursor and fragment ions. Two missed cleavages were allowed, and the minimum peptide length was set to four amino acids. The second peptide search was enabled. Variable modifications include lysine propionylation (+56.026215 Da), monomethylation-propionylation (+70.041865 Da), dimethylation (+28.031300 Da), trimethylation (+42.046950 Da), acetylation (+42.010565 Da), malonylation (+86.000394 Da), and succinylation (+100.016044 Da). N-terminal PIC labeling (+119.037114 Da) was set as a fixed modification (Noberini et al., 2021). To reduce the search time and the rate of false positives, which increases with a higher number of variable modifications included in the database search, the raw data were analyzed through multiple parallel MaxQuant jobs (Bremang et al., 2013), setting different combinations of variable modifications. Peptides identified by MaxQuant with Andromeda score higher than 50 and localization probability score higher than 0.75 were quantitated, either manually or by using a version of the EpiProfile 2.0 software (Yuan et al., 2018) adapted to the analysis of histones from *Aspergillus* strains. Identifications and retention times were used to guide the manual quantification of each modified peptide using QualBrowser version 2.0.7 (Thermo Scientific). Site assignment was evaluated from MS2 spectra using QualBrowser and MaxQuant Viewer. Extracted ion chromatograms were constructed for each doubly charged precursor, based on its m/z value, using a mass tolerance of 10 ppm. For each modified histone peptide, the relative abundance was estimated by dividing the area under the curve (AUC) of each modified peptide by the sum of the areas corresponding to all the observed forms of that peptide (Pesavento et al., 2006). The MS proteomics data have been deposited to the ProteomeXchange Consortium (Vizcaíno et al., 2014) *via* the PRIDE partner repository with the dataset identifier PXD033478.

PCA figures were generated by sklearn.decomposition.PCA of Sklearn (Pedregosa et al., 2011) in Python, heatmap and point plots were made using Seaborn (Waskom, 2021) in Python. To compare the relative abundance of each histone PTM among different species/strains, we first used 'bioinfokit.stat.oanova' to perform the one-way ANOVA test, then used 'bioinfokit.analys.stat.tukey_hsd' to perform the post-hoc Tukey HSD (Honestly Significant Difference) test in python (Bedre, 2020). We used $\alpha = 0.05$ and $\alpha/2 = 0.025$ as thresholds for a significant difference in the ANOVA and Tukey HSD tests, respectively.

3. Results and discussion

The study of histone PTMs in filamentous fungi has mostly been restricted to targeted analyses based on knowledge from other organisms. However, the discovery of novel histone PTMs and their potential co-occurrence on a single nucleosome requires the use of untargeted strategies. We here applied a quantitative MS approach to identify the (co-)occurrence of histone PTMs and to quantify their relative abundance in three *Aspergillus* species: *A. niger*, *A. fumigatus*, and *A. nidulans*, which belong to distinct taxonomic sections (Barrett et al., 2020). Protein sequences of histones H2A, H2B, H3, and H4 from human, yeast, and the three Aspergilli show very high levels of sequence conservation, especially in the core domains of all histone proteins that fold into the characteristic bulk octamer around which the DNA strand wraps, as well as in the N-terminal tails of H3 and H4 that protrude from the surface of the nucleosome and harbors most of histone PTMs (Mersfelder and Parthun, 2006) (Fig. 1). The majority of well-described histone PTMs, *i.e.*, methylation and acetylation, as well as less abundant PTMs such as crotonylation and ubiquitination predominantly occur on lysine residues, but histone PTMs can also occur on other residues such as serine, threonine, and arginine (Grau-Bové et al., 2022). For histone protein H3, we observed the conservation of all lysine residues in human, yeast, and Aspergilli, except for two additional lysine residues at positions 121 and 125 in *S. cerevisiae* (Fig. 1). On these two residues, Cul8/Rtt101, an enzyme that is thought to be specific to *S. cerevisiae* as no homolog has yet been found in human or other fungi, can introduce histone ubiquitylation and thereby regulate nucleosome assembly (Han et al., 2013; Young et al., 2020). We similarly observed limited variation in the N-terminal tail of histone protein H4 and the global core domains of H2A and H2B, and most of the polymorphism occurs on amino acid residues that are not known to carry any histone PTM.

3.1. Histone protein extraction and digestion for MS-based analyses

We adapted a well-established protocol for human primary cells (Noberini et al., 2020) to specifically extract histone proteins from filamentous fungi with three additional steps (freeze drying, grinding, and homogenization) for efficient disruption of fungal cell walls and release of nuclei (Zhang et al., 2022; Zhang et al., 2021) (Fig. 2A). We extracted histone proteins in three biological replicates from the three *Aspergillus* species; two strains of *A. nidulans* (Wtpaba and TN02A25) were cultured on YAG medium, while *A. niger* strain NRRL3 and *A. fumigatus* strain Af293 were grown on MEA medium (Fig. 2B). After visualizing the extracted histone protein on SDS-PAGE gel, bands ranging from 10,000 to 16,000 Dalton, which correspond to the size of histone proteins (Zhou et al., 2020), were cut for in-gel digestion (Fig. 2C). We used lysine derivatization with propionic anhydride on unmodified and mono-methylated lysines, followed by trypsin digestion and peptide N-terminal derivatization with phenyl isocyanate (PIC) to obtain histone peptides of amino acids length required for MS analysis. This method allows performing an 'Arg-C-like' digestion of histone proteins directly in the gel, which is the ideal digestion pattern for histone PTM analyses (Noberini et al., 2021). In addition, because the derivatization occurs only on unmodified or monomethylated lysines, but not on di- or tri-methylated residues, it allows better discrimination of isobaric peptides (Noberini et al., 2021). The N-terminal derivatization with PIC also aids in the detection of small and hydrophilic peptides, as well as the chromatographic separation of differentially acetylated peptides, as described previously (Noberini et al., 2021; Maile et al., 2015). After digestion of isolated histone proteins from Aspergilli, we detected 20 different peptides from the four core histone proteins and three peptides from the histone protein variant H2A.Z (Fig. 1, Table S1). These peptides cover most of the lysine residues that are known to harbor histone PTMs.

3.2. MS uncovers histone PTMs in three Aspergillus species

MS analyses resulted in the detection of 23 individual histone PTMs, as well as 23 distinct co-occurrence patterns of multiple histone PTMs that occur on the same peptide (Fig. 3, Table S1). We did not detect any histone PTM on histone variant H2A.Z and histone H2A, but we were able to detect acetylation on K92 and co-occurrent mono-methylations on K98 and K99 on histone protein H2B (Table S1). These PTMs correspond to histone PTMs H2BR79ac (R: arginine) and H2BK85me1R86me1 in human, yet the functions of these PTMs are

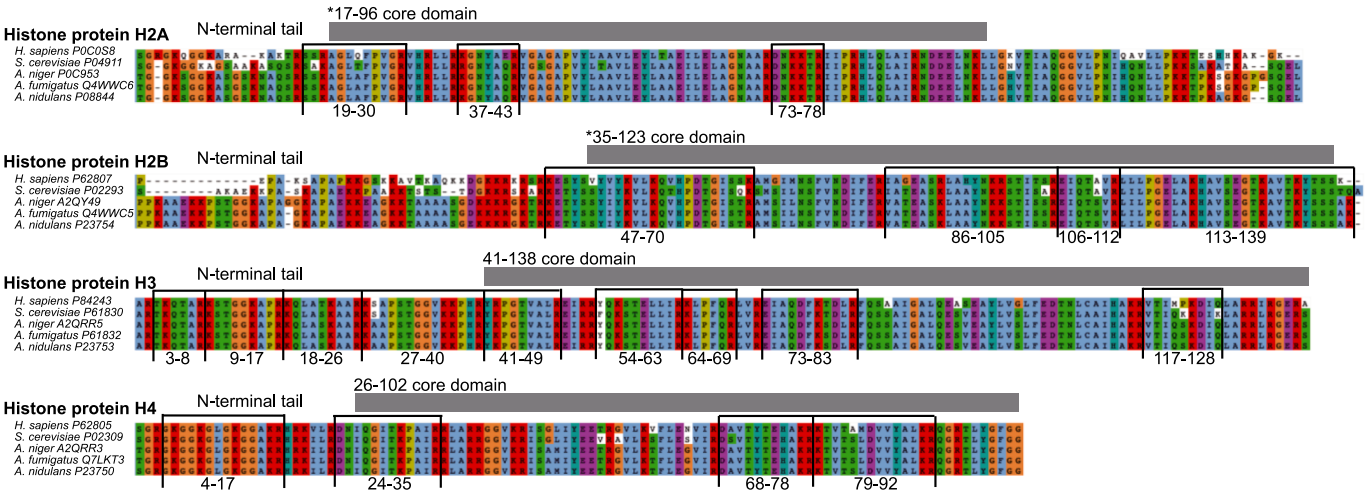

Fig. 1. Histone proteins are well conserved in Aspergilli. Sequence alignment of histone proteins from human (H2A: P0C0S8, H2B: P62807, H3: P84243, and H4: P62805), yeast (*S. cerevisiae*, H2A: P04911, H2B: P02293, H3: P61830, and H4: P02309), and *A. niger* (H2A: P0C953, H2B: A2QY49, H3: A2QRR5, and H4: A2QRR3), *A. fumigatus* (H2A: Q4WWC6, H2B: Q4WWC5, H3: P61832, and H4: Q7LKT3) and *A. nidulans* (H2A: P08844, H2B: P23754, H3: P23753, and H4: P23750), retrieved from UniProt database. The highly conserved globular histone core regions are highlighted by grey boxes with numbers indicating their position in human histone proteins with the symbol * showing the mismatch of the positions between human and Aspergilli histone proteins H2A and H2B caused by the poor alignment of the N-terminal tails. Peptides detected by MS in this study are labeled by black lines (Table S1), and their relative positions in Aspergilli histone proteins are indicated.

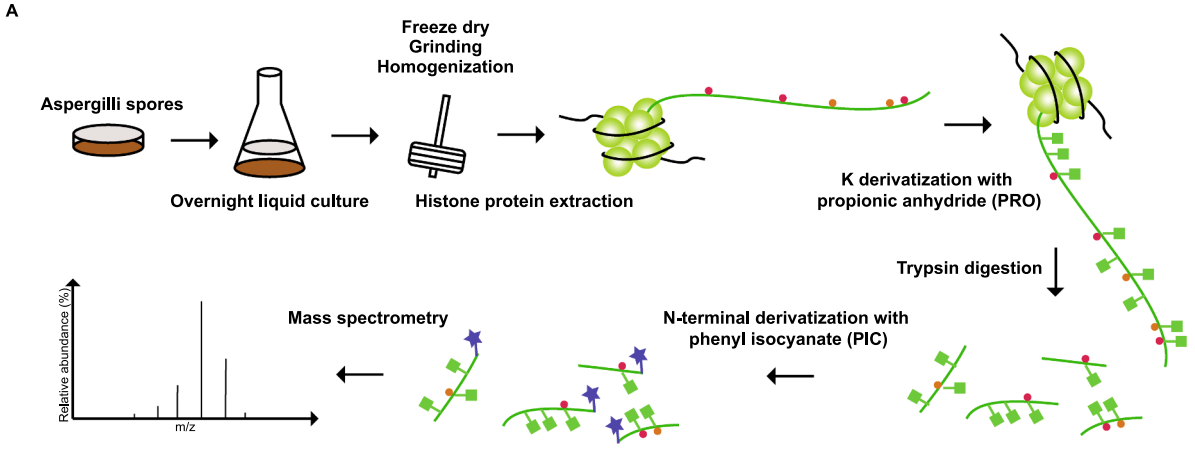

B

Species	*A. fumigatus*	*A. niger*	*A. nidulans*	
Strain	Af293	NRRL3	Wtpaba	TN02A25
Medium	MEA	MEA	YAG	YAG
Number of replicates	3	3	3	3

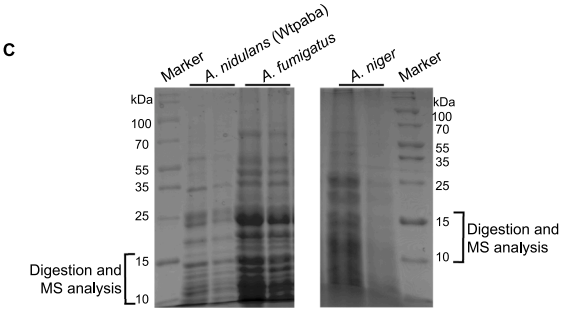

Fig. 2. Histone proteins extraction for MS-based analysis of histone PTMs in Aspergilli. A. Schematic diagram of the experimental setup and workflow applied in this work. **B.** Summary of *Aspergillus* strains' genetic background and culture conditions. The number of biological replicates for each condition is indicated. **C.** Histone proteins were extracted from the different *Aspergillus* species, and samples were visualized on the 17% SDS-PAGE gel. The region ranging from 10,000 to 16,000 Dalton was cut for the in-gel digestion step.

unknown (Gnesutta et al., 2013). For histone PTMs on histone proteins H3 and H4 in Aspergilli, we successfully detected methylations on histone H3 at lysines 4, 9, 36, and 79, acetylation on histone H3 at lysines 9, 14, 18, 23, 27, and 56, and histone H4 at lysines 5, 8, 12, 16, and 31 (Fig. 3). All these modifications have previously been reported in human (Pesavento et al., 2006; Barski et al., 2007), Arabidopsis (Scheid et al., 2022); *S. cerevisiae* (Abshiru et al., 2016), and in a few filamentous fungi (Collemare and Seidl, 2019; Freitag, 2017; Brosch et al., 2008). However, it is to our knowledge the first time that H3K79me1, H3K79me2, and H4K31ac are detected experimentally in Aspergilli (Fig. 3). Consistently with the occurrence of these histone PTMs, their catalytic enzymes, Dot1 (Disruptor of telomeric silencing 1) for H3K79me and

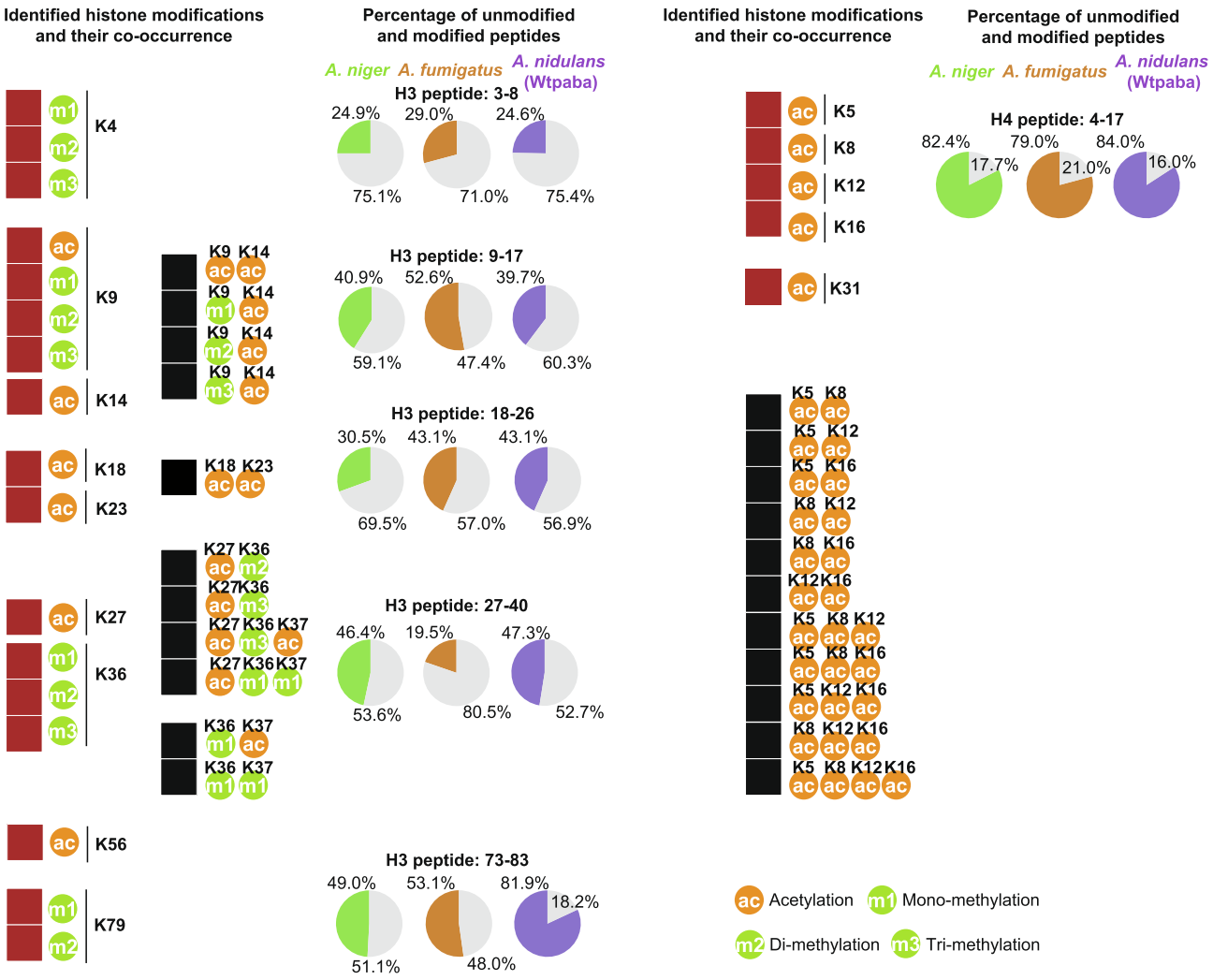

Fig. 3. Identification of single and co-occurrent histone PTMs in Aspergilli. The red boxes show the identification of histone mono-, di-, and tri-methylation and acetylation while the black boxes show their co-occurrences in Aspergilli. Pie charts show the average relative abundance of unmodified peptides compared with modified peptides for each *Aspergillus* species. Unmodified peptides are shown in gray, and green, orange, as well as purple representing the proportion of modified peptides in *A. niger*, *A. fumigatus*, and *A. nidulans* (strain Wtpaba), respectively. (For interpretation of the references to color in this figure legend, the reader is referred to the web version of this article.)

Gcn5 for H4K31ac were firstly identified in *S. cerevisiae* (van Leeuwen et al., 2002) and the human parasite *Toxoplasma* (Sindikubwabo et al., 2017), respectively, and then found to be conserved across the fungal genus *Aspergillus* in our previous study (Zhang et al., 2022). Our analysis could not differentiate between the two H4 variants found in Aspergilli because they only differ by two residues (Cheng et al., 2003; Grant et al., 1999; Fig. 1), which are inside the histone core domain that was not detected.

While we detected most of the known PTMs as well as a few additional ones for the first time in Aspergilli, we did not detect some histone PTMs which were expected to occur. Several reasons can explain these observations. First, PTMs might not be identified because they are under the detection threshold used in both the instrument and analysis pipeline. This reason likely explains why we only detected abundant histone methylations and acetylations, but not less-abundant ones, e.g., H3S10P (S: serine and P: phosphorylation) and H3R2me, which have been reported in Aspergilli (Cheng et al., 2003). The abundance of certain expected PTMs like H3K79me3, H3K4ac, and H3K36ac could be higher and detectable under different growth conditions or developmental stages. Second, these PTMs are true absences in Aspergilli. We were not able to detect any methylation on H3K27, H4K5, H4K8, and H4K12 (Figure S1), which is expected due to the absence in Aspergilli of their catalytic enzymes, PRC2 (Freitag, 2017; Zhang et al., 2022) and SET5 (Zhang et al., 2022) (Figure S2), respectively. Third, the mutual exclusivity of different histone PTMs on the same residue could lead to biased occupancy by only one histone PTM. For instance, apart from H3K9, either acetylation or methylation was detected on H3 lysines (Fig. 3 and Figure S1). Such an explanation would indicate very homogenous samples regarding their chromatin status and PTMs. Last, antagonistic relationships between histone PTMs might contribute to some absences. For example, H4K16ac prevents H4K20me (Nishioka et al., 2002), explaining why we could detect the former but not the latter histone PTM in Aspergilli.

We also detected the co-occurrence of multiple histone PTMs on the same peptide (Fig. 3). For example, we observed the co-occurrence of acetylations on different residues in the same peptide such as H3K9acK14ac, H3K18acK23ac, and H4 lysines 5, 8, 12, and 16 harboring acetylations at the same time on two, three, or four residues (Fig. 3). Acetylation can also co-occur with methylation, such as H3K9me1/2/3K14ac, H3K27acK36me2/3, and H3K36me1K37ac, while H3K36me1 can co-occur with another mono-methylation on H3K37 (Fig. 3). The detection and functional characterization of some of these co-occurrent patterns have been performed in several model species. For instance, in mouse, H3K9meK14ac has a role in gene silencing

(Jurkowska et al., 2017). Accordingly, double replacements of K9 and K14 by arginine residues on histone H3 lead to the missing acetylations on these two locations and down-regulation of penicillin, sterigmatocystin, and orsellinic acid in *A. nidulans* (Nützmann et al., 2013). H3K18acK23ac was first reported to be acetylated by SAGA/ADA complex in *S. cerevisiae* (Grant et al., 1999) and then detected in human (Han et al., 2021). The investigation in *S. cerevisiae* of the combinatorial effect of acetylation on H4 lysines 5, 8, 12, and 16 showed that they are redundant and function together as a group to induce gene activation instead of forming distinct combinational patterns (Dion et al., 2005). Even though the co-occurrence of histone PTMs has not yet been systematically studied, our data as well as the results from other model systems, such as human or mouse, provide valuable clues for the possible functions of co-occurring histone PTMs in gene regulation in Aspergilli.

Although relative abundances only represent an indication of the absolute abundance of a modification as peptide detection by MS is affected by the peptide physicochemical properties and the digestion strategy (Lin et al., 2014), our data shows that the majority of detected histone H3 peptides is unmodified, while histone protein H4 exhibits a high percentage (79%-84%) of acetylated peptides in all three Aspergilli (Fig. 3). According to a recent study, the newly synthesized histones are modified within 1.5 h for histones H2A and H2B, and 3.5 h for histones H3 and H4 (Flury et al., 2023). In our study, we cultured all Aspergilli strains at the same time and observed no difference in their growth

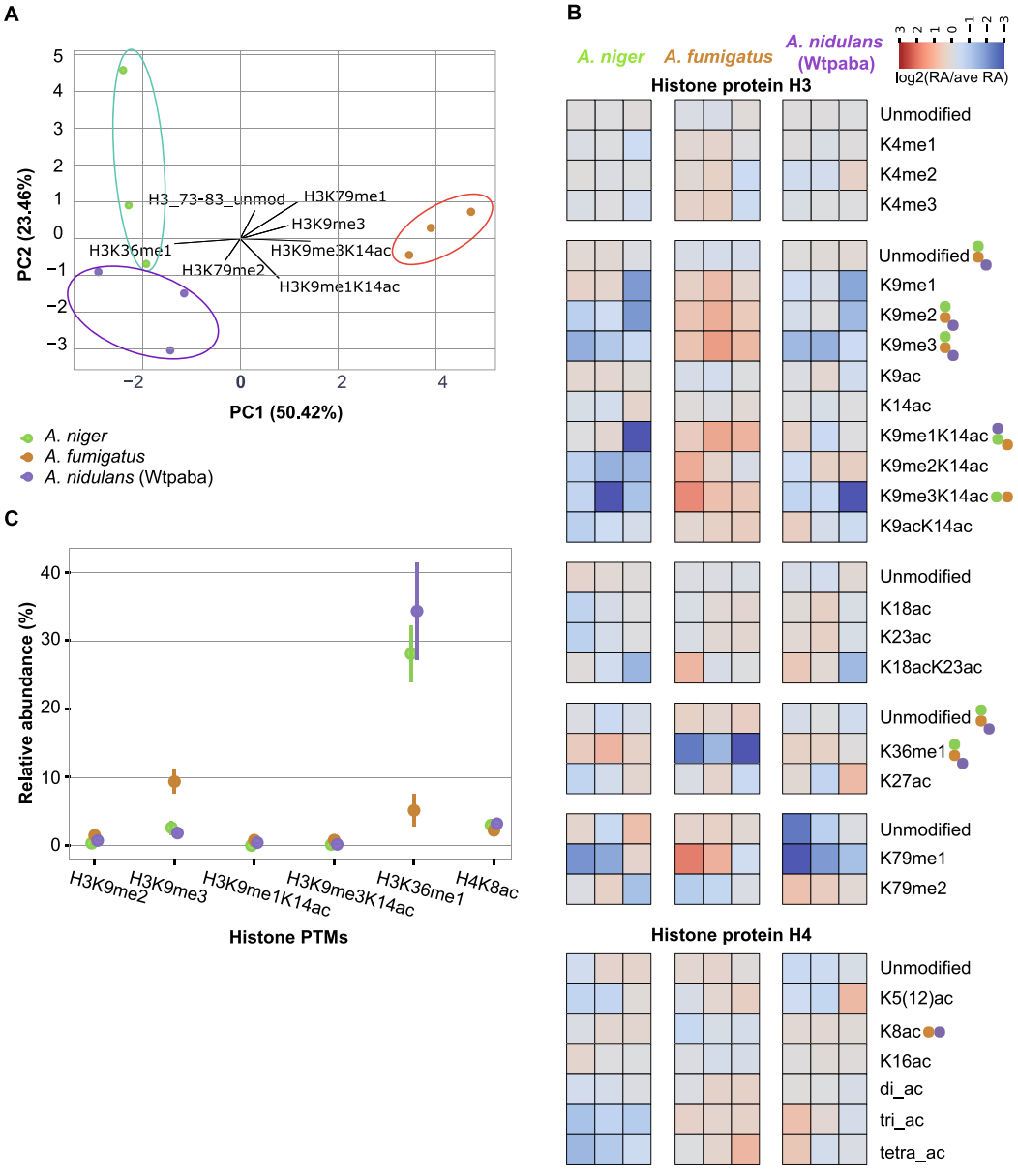

Fig. 4. Quantification of histone PTMs in three *Aspergillus* species. A. Principal component analysis (PCA) of three Aspergilli based on their relative abundance of histone PTMs (Table S3). **B.** Quantitative comparison of all histone PTMs detected by MS. The heatmap displays red or blue color boxes according to the $\log_2$(relative abundance/average of relative abundance) of different peptides in Aspergilli. 'Di-ac' indicates H4K5acK8ac, H4K5acK12ac, H4K5acK16ac, H4K8acK16ac, and H4K12acK16ac; 'tri-ac' means H4K5acK8ac12ac, H4K5acK8acK16ac, H4K5acK12acK16ac, and H4K8acK12acK16ac; and 'tetra-ac' indicates H4K5acK8ack12acK16ac. For each histone PTM between the three Aspergilli species, we applied an ANOVA test and Tukey HSD tests to determine significant differences. We used p-value = 0.05 as the threshold for a significant difference in the ANOVA test and p-value = 0.025 in the Tukey HSD test. Colored dots indicate significant differences between represented species. **C.** Relative abundance of histone PTMs that are significantly different. Points show the average relative abundance and lines indicate standard deviation. (For interpretation of the references to color in this figure legend, the reader is referred to the web version of this article.)

among replicates. Different growth rates cannot explain the observed differences because one would expect the proportion of modified peptides to be consistent within a given species, which is not the case here. Indeed, the pattern we mentioned above is similar among the three species, with only a few observable differences. Fewer H3 peptides 18–26 are modified in *A. niger* (30% vs 43% in both *A. nidulans* and *A. fumigatus*), suggesting a lower abundance of H3K18ac and/or H3K23ac in this species. In contrast, *A. nidulans* exhibit more modified H3 peptides 73–83 (82% vs 49–53% in the other species), suggesting an enrichment in H3K79 methylation in this species. *A. fumigatus* differs from the two other species by having more modified H3 peptides 9–17 (53% vs 40–41%) and fewer modified H3 peptides 27–40 (19% vs 46–47%) (Fig. 3). These differences suggest a higher abundance of H3K9 and/or H3K14 PTMs and a lower abundance of H3K27, H3K36, and/or H3K37 PTMs in *A. fumigatus*. These results collectively suggest that, although the same histone PTMs are detected in all three species, their abundances likely differ.

3.3. *Aspergillus species differ in the relative abundance of histone PTMs*

To uncover quantitative differences between histone PTMs, we calculated the relative abundance of most histone PTMs in three *Aspergillus* species (*A. niger*, *A. fumigatus*, and *A. nidulans* (Wtpaba strain). Of note, a few modified peptides could not be quantified as their chromatographic peaks were of poor quality or could not be fully resolved for accurate quantification. We plotted the figure of Principal Component Analysis (PCA) (Fig. 4A) and observed that *Aspergillus* species are well separated, suggesting that the three Aspergilli indeed differ quantitatively in their histone PTMs. These differences could be caused by differences in growth conditions (Fig. 2B). However, we observed that even though *A. fumigatus* and *A. niger* were grown on the same medium compared with *A. nidulans*, *A. fumigatus* was more distinct from *A. nidulans* and *A. niger*. These distinctions suggest that the observed differences are not related to the different media but seem to be consistent with their taxonomic relationships. Specifically, *A. fumigatus* harbors significantly more H3K9 methylations, either alone or co-occurring with H3K14ac, and it has significantly less H3K36me1 compared to the other two Aspergilli (Fig. 4B, Table S3). *A. fumigatus* also appears to have a trend of being enriched in H3K79me1 compared to *A. nidulans* (p-value: 0.080789) and *A. niger* (p-value: 0.165426) (Figs. 3 and 4B, Table S3). In contrast, H3K9me1/2K14ac showed lower abundance in *A. niger* compared to the other two species, and H4K8ac was significantly higher in *A. fumigatus* compared to *A. nidulans*. There are also trends indicating that *A. niger* contains fewer H3K18ac and H3K23ac while *A. nidulans* appears particularly rich in H3K79me2 and poor in H3K79me1 (Figs. 3 and 4B). The observed differences suggest that *A. fumigatus* exhibit more heterochromatin- linked modifications compared to the other two species as it harbors more H3K9me1/2/3 linked with constitutive heterochromatin (Lachner et al., 2001) and H3K9meK14ac associated with triggering gene silencing (Jurkowska et al., 2017). For euchromatin, *A. fumigatus* uses more H3K79me1 and the combination of acetylations on diverse lysines of histone protein H4, while *A. niger* and *A. nidulans* harbors more H3K36me1 (Fig. 4B). Even though we observed no qualitative difference in histone PTMs among three Aspergilli, these species differ quantitatively in specific histone PTM abundances, suggesting that the three populations (and their replicates) were very homogenous and in a similar state and they used a mix of marks associated with gene activation and gene silencing. Yet, the absence or low abundance of histone PTMs like H3K4ac, H3K14me, or H3K36ac could indicate their important roles in gene regulation in other developmental stages.

3.4. *A. nidulans strains differ quantitatively in euchromatin marks*

To evaluate the intra-species variation in the relative abundance of histone PTMs, we compared the MS data of another *A. nidulans* strain (TN02A25) to Wtpaba (Fig. 5). In general, we observed that TN02A25 spurs the same type of histone PTMs as we observed in the other strains (Fig. 4B and 5C), indicating all Aspergilli tested in this study used the same histone code. However, the two strains show a few differences, already when only considering the percentage of unmodified versus modified peptides. The vast majority of detected histone H3 peptides were unmodified (>50%) and histone H4 peptides were highly acetylated in TN02A25 like the other strains (Fig. 4 and Fig. 5A). However, TN02A25 differs from Wtpaba in H3 peptides 27–40 (11% vs 47% modified peptides in Wtpaba) and 73–83 (46% vs 82% modified peptides in Wtpaba). These proportions in TN02A25 are similar to those found in *A. fumigatus* or *A. niger* and *A. fumigatus*, respectively (Fig. 3), and suggest that the two *A. nidulans* strains differ in histone PTM abundance on those peptides.

The quantitative comparison of histone PTMs between the two *A. nidulans* strains shows good separation in the PCA analysis (Fig. 5B). Consistent with previous results and analyses, TN02A25 exhibit significantly less H3K36me1 compared to the Wtpaba strain. We also observed a trend of enrichment in H3K79me2 and lower abundance in H3K79me1 in Wtpaba, which contributes to the difference between both strains (Fig. 5). In addition, H3K4me2, H3K9ac, H3K36me1, and H4di-ac (H4K5acK8ac, H4K5acK12ac, H4K5acK16ac, H4K8acK16ac, and H4K12acK16ac) exhibited significantly higher abundance in Wtpaba than TN02A25 (Fig. 5C-D, Table S4) and they are all related to regulation of euchromatin.

Moreover, we observed that intra-species variability can be as high as the inter-species variability as the histone PTM abundances of Wtpaba and TN02A25 are more related to *A. niger* and *A. fumigatus,* respectively (Fig. S3A, Table S5). Four single or co-occurrent histone PTMs, H3K36me1, H3K79me1, H3K9me3K14ac, and H3K9me1K14ac displayed the most distinct abundant patterns among the four strains, followed by H3K9me1, H3K9me2, and H3K18acK23ac being less abundant in *A. niger* compared to the other three strains (Fig. S3B). These marks showing distinct relative abundance agreed with the marks we pinpointed from both species and strain comparisons. Thus, the observed differences between species are likely a 'strain effect'. These differences could be due to the genotype of TN02A25 because the *nku* gene is deleted in this strain, which is known to influence chromatin structure. Including several strains in future studies of histone PTMs will determine how critical this mutation is for the observed intra-species variation.

The use of MS spectrometry is powerful to detect and quantify histone PTMs in filamentous fungi and this approach is needed to understand the chromatin status at different developmental stages. The present study focused on fungal mycelium cultured for 16 h in liquid medium, a particular stage that requires the expression of a specific set of genes and is expected to not favor the production of SMs. Similar future studies in Aspergilli at different developmental stages and different culture conditions will fully uncover quantitative variations in histone PTMs and might lead to identifying key PTMs for certain applications, such as the controlled activation of SM production. Finally, while this work has revealed quantitative differences between species and strains, it remains to determine whether they are due to different PTM abundance at the same loci, or whether they reflect a different number of loci covered by these PTMs, which would reflect activation or repression of different sets of genes. These future studies will contribute to understanding how single and co-occurring histone PTMs regulate gene expression in Aspergilli and more broadly in other filamentous fungi.

CRediT authorship contribution statement

Xin Zhang: Formal analysis, Investigation, Methodology, Visualization, Writing – original draft. **Roberta Noberini:** Formal analysis, Investigation, Methodology. **Alessandro Vai:** Formal analysis, Investigation, Methodology. **Tiziana Bonaldi:** Funding acquisition, Supervision, Resources. **Michael F. Seidl:** Conceptualization, Funding

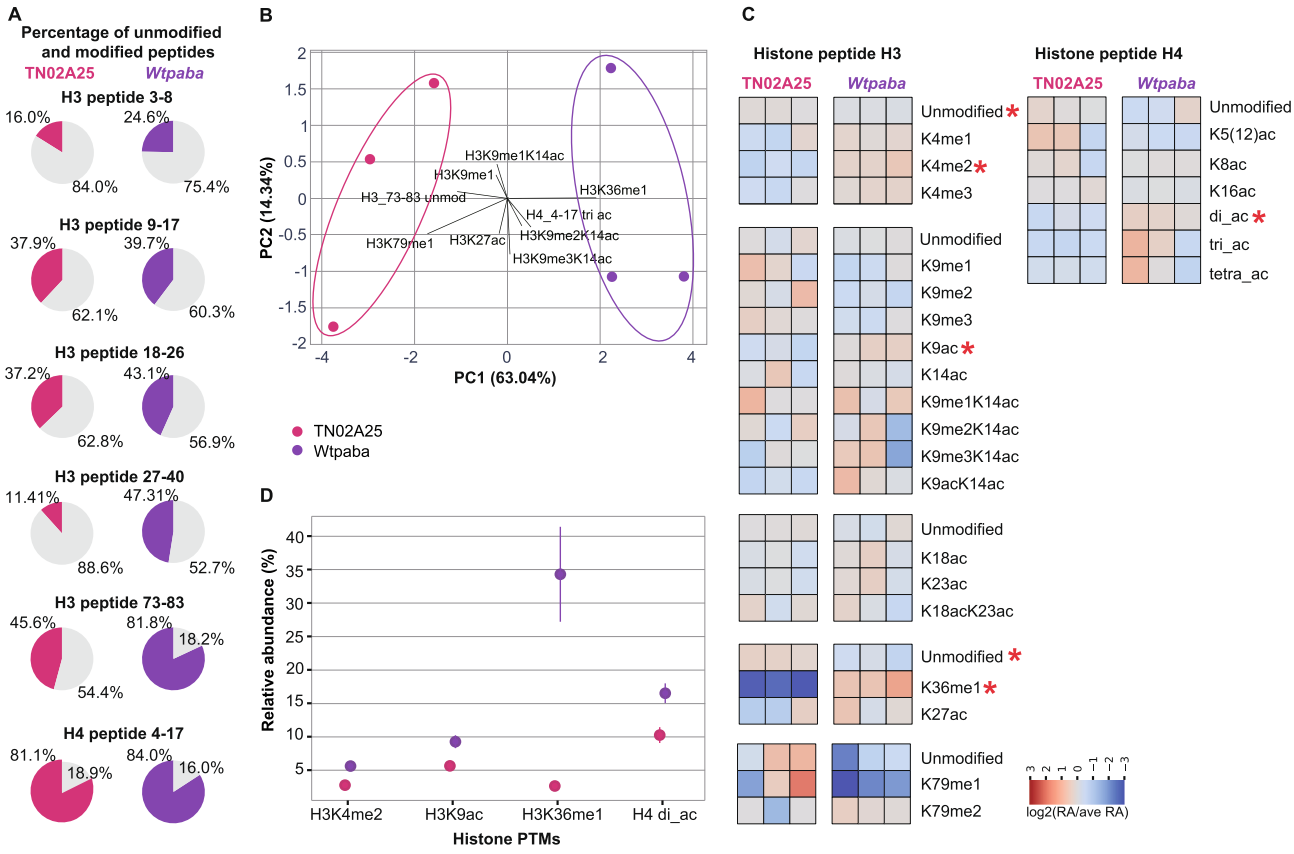

Fig. 5. Quantification of histone modifications in two *A. nidulans* strains. A. The average relative abundance of unmodified peptides compared with modified peptides. Grey represents the unmodified peptide percentage in the pie chart, while pink and purple represent the modified peptide percentage of TN02A25 and Wtpaba *A. nidulans* strains, respectively. **B.** Principal component analysis (PCA) of two strains based on their relative abundance of histone PTMs. **C.** Quantitative comparison of all histone PTMs detected by MS. The heatmap displays red or blue color boxes according to the $\log_2$(relative abundance/average of relative abundance) of different peptides in two *A. nidulans* strains. 'Di-ac' indicates H4K5acK8ac, H4K5acK12ac, H4K5acK16ac, H4K8acK16ac, and H4K12acK16ac; 'tri-ac' means H4K5acK8ac12ac, H4K5acK8acK16ac, H4K5acK12acK16ac, and H4K8acK12acK16ac; and 'tetra-ac' indicates H4K5acK8ack12acK16ac. ANOVA test and Tukey HSD test were performed to show the significance of the difference of one histone modification between two strains when p-value < 0.05 in the ANOVA test and p-value < 0.025 in the Tukey HSD test. Red stars indicate significant differences. **D.** The relative abundance of the top four histone modifications that are significantly different. Points are average relative abundance and lines are standard deviations. (For interpretation of the references to color in this figure legend, the reader is referred to the web version of this article.)

acquisition, Methodology, Project administration, Supervision, Visualization, Writing – original draft. **Jérôme Collemare:** Conceptualization, Funding acquisition, Methodology, Project administration, Supervision, Visualization, Writing – original draft.

Declaration of Competing Interest

The authors declare that they have no known competing financial interests or personal relationships that could have appeared to influence the work reported in this paper.

Data availability

Data statement: All supporting data, code, and protocols have been provided within the article or through supplementary data files. Supplementary material is available with the online version of this article. The MS results are deposited in the PRIDE database with the dataset identifier PXD033478.

Acknowledgments

We thank Jos Houbraken for providing *A. fumigatus* strain and Joseph Strauss for providing two *A. nidulans* strains.

Funding information

Xin Zhang is funded by the Chinese Scholarship Council (CSC) (201907720028). This work was supported by EPIC-XS, project number 823 839, funded by the Horizon 2020 programme of the European Union.

Appendix A. Supplementary material

Supplementary data to this article can be found online at https://doi.org/10.1016/j.fgb.2023.103800.

References

Abshiru, N., Rajan, R.E., Verreault, A., Thibault, P., 2016. Unraveling Site-Specific and Combinatorial Histone Modifications Using High-Resolution Mass Spectrometry in Histone Deacetylase Mutants of Fission Yeast. J. Proteome Res. 15 (7), 2132–2142.

Adlakha, A., Armstrong-James, D.A.J., Lenhard, B., 2016. T1 calcineurin inhibition impairs the dendritic cell transcriptional response to *Aspergillus fumigatus* infection in lung transplant recipients. BMJ Publishing Group Ltd.

Barrett, K., Jensen, K., Meyer, A.S., Frisvad, J.C., Lange, L., 2020. Fungal secretome profile categorization of CAZymes by function and family corresponds to fungal phylogeny and taxonomy: Example *Aspergillus* and *Penicillium*. Sci. Rep. 10 (1), 1–12.

Barski, A., Cuddapah, S., Cui, K., Roh, T.-Y., Schones, D.E., Wang, Z., et al., 2007. High-resolution profiling of histone methylations in the human genome. Cell 129 (4), 823–837.

Bhaumik, S.R., Smith, E., Shilatifard, A., 2007. Covalent modifications of histones during development and disease pathogenesis. Nat. Struct. Mol. Biol. 14 (11), 1008–1016.

Bicocca, V.T., Ormsby, T., Adhvaryu, K.K., Honda, S., Selker, E.U., 2018. ASH1-catalyzed H3K36 methylation drives gene repression and marks H3K27me2/3-competent chromatin. Elife 7, 1–19.
Bremang, M., Cuomo, A., Agresta, A.M., Stugiewicz, M., Spadotto, V., Bonaldi, T., 2013. Mass spectrometry-based identification and characterisation of lysine and arginine methylation in the human proteome. Mol. Biosyst. 9 (9), 2231–2247.
Brosch, G., Loidl, P., Graessle, S., 2008. Histone modifications and chromatin dynamics: A focus on filamentous fungi. FEMS Microbiol. Rev. 32 (3), 409–439.
Cánovas, D., Marcos, A.T., Gacek, A., Ramos, M.S., Gutiérrez, G., Reyes-Domínguez, Y., et al., 2014. The histone acetyltransferase GcnE (GCN5) plays a central role in the regulation of *Aspergillus* asexual development. Genetics 197 (4), 1175–1189.
Chen, X., Wu, L., Lan, H., Sun, R., Wen, M., Ruan, D., et al., 2022. Histone acetyltransferases MystA and MystB contribute to morphogenesis and aflatoxin biosynthesis by regulating acetylation in fungus *Aspergillus flavus*. Environ. Microbiol. 24 (3), 1340–1361.
Cheng, J., Park, T.-S., Chio, L.-C., Fischl, A.S., Ye, X.S., 2003. Induction of apoptosis by sphingoid long-chain bases in *Aspergillus nidulans*. Mol. Cell. Biol. 23 (1), 163–177.
Colabardini, A.C., Wang, F., Miao, Z., Pardeshi, L., Valero, C., de Castro, P.A., et al., 2022. Chromatin profiling reveals heterogeneity in clinical isolates of the human pathogen *Aspergillus fumigatus*. PLoS Genet. 18, 1–36.
Collemare, J., Seidl, M.F., 2019. Chromatin-dependent regulation of secondary metabolite biosynthesis in fungi: is the picture complete? FEMS Microbiol. Rev. 43 (6), 591–607.
Connolly, L.R., Smith, K.M., Freitag, M., 2013. The *Fusarium graminearum* histone H3 K27 methyltransferase KMT6 regulates development and expression of secondary metabolite gene clusters. PLoS Genet. 9 (10), e1003916.
De Souza, C.P.C., Osmani, A.H., Wu, L.-P., Spotts, J.L., Osmani, S.A., 2000. Mitotic histone H3 phosphorylation by the NIMA kinase in *Aspergillus nidulans*. Cell 102 (3), 293–302.
Dion, M.F., Altschuler, S.J., Wu, L.F., Rando, O.J., 2005. Genomic characterization reveals a simple histone H4 acetylation code. Proc. Natl. Acad. Sci. 102 (15), 5501–5506.
Farooq, Z., Banday, S., Pandita, T.K., Altaf, M., 2016. The many faces of histone H3K79 methylation. Mutat. Res. – Rev. Mutat. Res. 768, 46–52.
Flury, V., Reverón-Gómez, N., Alcaraz, N., Stewart-Morgan, K.R., Wenger, A., Klose, R.J., et al., 2023. Recycling of modified H2A–H2B provides short-term memory of chromatin states. Cell 1–16.
Freitag, M., 2017. Histone Methylation by SET Domain Proteins in Fungi. Annu. Rev. Microbiol. 71, 413–439.
Gacek-Matthews, A., Noble, L.M., Gruber, C., Berger, H., Sulyok, M., Marcos, A.T., et al., 2015. KdmA, a histone H3 demethylase with bipartite function, differentially regulates primary and secondary metabolism in *Aspergillus nidulans*. Mol. Microbiol. 96 (4), 839–860.
Gacek-Matthews, A., Berger, H., Sasaki, T., Wittstein, K., Gruber, C., Lewis, Z.A., et al., 2016. KdmB, a Jumonji Histone H3 Demethylase, Regulates Genome-Wide H3K4 Trimethylation and Is Required for Normal Induction of Secondary Metabolism in *Aspergillus nidulans*. PLoS Genet. 12 (8), 1–29.
Gates, L.A., Shi, J., Rohira, A.D., Feng, Q., Zhu, B., Bedford, M.T., et al., 2017. Acetylation on histone H3 lysine 9 mediates a switch from transcription initiation to elongation. J. Biol. Chem. 292 (35), 14456–14472.
Gnesutta, N., Nardini, M., Mantovani, R., 2013. The H2A/H2B-like histone-fold domain proteins at the crossroad between chromatin and different DNA metabolisms. Transcription. 4 (3), 114–119.
Grant, P.A., Eberharter, A., John, S., Cook, R.G., Turner, B.M., Workman, J.L., 1999. Expanded lysine acetylation specificity of Gcn5 in native complexes. J. Biol. Chem. 274 (9), 5895–5900.
Grau-Bové, X., Navarrete, C., Chiva, C., Pribasnig, T., Antó, M., Torruella, G., et al., 2022. A phylogenetic and proteomic reconstruction of eukaryotic chromatin evolution. Nat. Ecol. Evol. 1–17.
Guillemette, B., Drogaris, P., Lin, H.H.S., Armstrong, H., Hiragami-Hamada, K., Imhof, A., et al., 2011. H3 lysine 4 is acetylated at active gene promoters and is regulated by H3 lysine 4 methylation. PLoS Genet. 7 (3).
Han, X., Tian, M., Shliaha, P.V., Zhang, J., Jiang, S., Nan, B., et al., 2021. Real-world particulate matters induce lung toxicity in rats fed with a high-fat diet: Evidence of histone modifications. J. Hazard. Mater. 416, 126182.
Han, J., Zhang, H., Zhang, H., Wang, Z., Zhou, H., Zhang, Z., 2013. A Cul4 E3 ubiquitin ligase regulates histone hand-off during nucleosome assembly. Cell 155 (4), 817.
He, F., 2011. Bradford protein assay. Bio-protocol. 45.
Henikoff, S., Shilatifard, A., 2011. Histone modification: cause or cog? Trends Genet. 27 (10), 389–396.
Huang, H., Lin, S., Garcia, B.A., Zhao, Y., 2015. Quantitative proteomic analysis of histone modifications. Chem. Rev. 115 (6), 2376–2418.
Janevska, S., Baumann, L., Sieber, C.M.K., Münsterkötter, M., Ulrich, J., Kämper, J., et al., 2018. Elucidation of the two H3K36me3 histone methyltransferases Set2 and Ash1 in *Fusarium fujikuroi* unravels their different chromosomal targets and a major impact of Ash1 on genome stability. Genetics 208, 153–171.
Johnson, L., Mollah, S., Garcia, B.A., Muratore, T.L., Shabanowitz, J., Hunt, D.F., et al., 2004. Mass spectrometry analysis of Arabidopsis histone H3 reveals distinct combinations of post-translational modifications. Nucleic Acids Res. 32 (22), 6511–6518.
Jurkowska, R.Z., Qin, S., Kungulovski, G., Tempel, W., Liu, Y., Bashtrykov, P., et al., 2017. H3K14ac is linked to methylation of H3K9 by the triple Tudor domain of SETDB1. Nat. Commun. 8 (1), 1–13.
Lachner, M., O'Carroll, D., Rea, S., Mechtler, K., Jenuwein, T., 2001. Methylation of histone H3 lysine 9 creates a binding site for HP1 proteins. Nature 410 (6824), 116–120.
Lin, S., Wein, S., Gonzales-Cope, M., Otte, G.L., Yuan, Z.F., Afjehi-Sadat, L., et al., 2014. Stable-isotope-labeled histone peptide library for histone post-translational modification and variant quantification by mass spectrometry. Mol. Cell. Proteomics 13 (9), 2450–2466.
Luger, K., Mader, A.W., Richmond, R.K., Sargent, D.F., Richmond, T.J., 1997. Crystal structure of the nucleosome resolution core particle at 2.8 Å. Nature 389, 251–260.
Maile, T.M., Izrael-Tomasevic, A., Cheung, T., Guler, G.D., Tindell, C., Masselot, A., et al., 2015. Mass spectrometric quantification of histone post-translational modifications by a hybrid chemical labeling method. Mol. Cell. Proteomics 14 (4), 1148–1158.
Mersfelder, E.L., Parthun, M.R., 2006. The tale beyond the tail: Histone core domain modifications and the regulation of chromatin structure. Nucleic Acids Res. 34 (9), 2653–2662.
Nishioka, K., Rice, J.C., Sarma, K., Erdjument-Bromage, H., Werner, J., Wang, Y., et al., 2002. PR-Set7 is a nucleosome-specific methyltransferase that modifies lysine 20 of histone H4 and is associated with silent Chromatin. Mol. Cell 9 (6), 1201–1213.
Noberini, R., Restellini, C., Savoia, E.O., Bonaldi, T., 2020. Enrichment of histones from patient samples for mass spectrometry-based analysis of post-translational modifications. Methods 184, 19–28.
Noberini, R., Savoia, E.O., Brandini, S., Greco, F., Marra, F., Bertalot, G., et al., 2021. Spatial epi-proteomics enabled by histone post-translational modification analysis from low-abundance clinical samples. Clin. Epigenetics 13 (1), 1–16.
Nützmann, H.-W., Reyes-Dominguez, Y., Scherlach, K., Schroeckh, V., Horn, F., Gacek, A., et al., 2011. Bacteria-induced natural product formation in the fungus Aspergillus nidulans requires Saga/Ada-mediated histone acetylation. Proc. Natl. Acad. Sci. 108 (34), 14282–14287.
Nützmann, H.-W., Fischer, J., Scherlach, K., Hertweck, C., Brakhage, A.A., 2013. Distinct amino acids of histone H3 control secondary metabolism in *Aspergillus nidulans*. Appl. Environ. Microbiol. 79 (19), 6102–6109.
Pedregosa, F., Varoquaux, G., Gramfort, A., Michel, V., Thirion, B., Grisel, O., et al., 2011. Scikit-learn: Machine learning in Python. J. Mach. Learning Res. 12, 2825–2830.
Pesavento, J.J., Mizzen, C.A., Kelleher, N.L., 2006. Quantitative analysis of modified proteins and their positional isomers by tandem mass spectrometry: human histone H4. Anal. Chem. 78 (13), 4271–4280.
Pokholok, D.K., Harbison, C.T., Levine, S., Cole, M., Hannett, N.M., Tong, I.L., et al., 2005. Genome-wide map of nucleosome acetylation and methylation in yeast. Cell 122 (4), 517–527.
Bedre, R., 2020. Reneshbedre/bioinfokit: Bioinformatics data analysis and visualization toolkit. 2020.
Reyes-Dominguez, Y., Narendja, F., Berger, H., Gallmetzer, A., Fernandez-Martin, R., Garcia, I., et al., 2008. Nucleosome positioning and histone H3 acetylation are independent processes in the *Aspergillus nidulans* prnD-prnB bidirectional promoter. Eukaryot. Cell 7 (4), 656–663.
Reyes-Dominguez, Y., Bok, J.W., Berger, H., Shwab, E.K., Basheer, A., Gallmetzer, A., et al., 2010. Heterochromatic marks are associated with the repression of secondary metabolism clusters in *Aspergillus nidulans*. Mol. Microbiol. 76 (6), 1376–1386.
Rountree, M.R., Selker, E.U., 2010. DNA methylation and the formation of heterochromatin in *Neurospora crassa*. Heredity 105 (1), 38–44.
Scheid, R., Dowell, J.A., Sanders, D., Jiang, J., Denu, J.M., Zhong, X., 2022. Histone Acid Extraction and High Throughput Mass Spectrometry to Profile Histone Modifications in *Arabidopsis thaliana*. Curr. Protocols. 2 (8), e527.
Shilatifard, A., 2006. Chromatin modifications by methylation and ubiquitination: implications in the regulation of gene expression. Annu. Rev. Biochem 75, 243–269.
Shinohara, Y., Kawatani, M., Futamura, Y., Osada, H., Koyama, Y., 2016. An overproduction of astellolides induced by genetic disruption of chromatin-remodeling factors in *Aspergillus oryzae*. J. Antibiot. 69 (1), 4–8.
Sindikubwabo, F., Ding, S., Hussain, T., Ortet, P., Barakat, M., Baumgarten, S., et al., 2017. Modifications at K31 on the lateral surface of histone H4 contribute to genome structure and expression in apicomplexan parasites. Elife 6, 1–34.
Tan, M., Luo, H., Lee, S., Jin, F., Yang, J.S., Montellier, E., et al., 2011. Identification of 67 histone marks and histone lysine crotonylation as a new type of histone modification. Cell 146 (6), 1016–1028.
van Holde, K.E., 1989. Chromatin structure and transcription. In: Chromatin. Springer, p. 355–408.
van Leeuwen, F., Gafken, P.R., Gottschling, D.E., 2002. Dot1p modulates silencing in yeast by methylation of the nucleosome core. Cell 109 (6), 745–756.
Vizcaíno, J.A., Deutsch, E.W., Wang, R., Csordas, A., Reisinger, F., Rios, D., et al., 2014. ProteomeXchange provides globally coordinated proteomics data submission and dissemination. Nat. Biotechnol. 32 (3), 223–226.
Waskom, M.L., 2021. Seaborn: statistical data visualization. J. Open Source Softw. 6 (60), 3021.
Wiemann, P., Sieber, C.M.K., Von Bargen, K.W., Studt, L., Niehaus, E.-M., Espino, J.J., et al., 2013. Deciphering the cryptic genome: genome-wide analyses of the rice pathogen *Fusarium fujikuroi* reveal complex regulation of secondary metabolism and novel metabolites. PLoS Pathog. 9 (6), e1003475.
Yamada, T., Fischle, W., Sugiyama, T., Allis, C.D., Grewal, S.I.S., 2005. The nucleation and maintenance of heterochromatin by a histone deacetylase in fission yeast. Mol. Cell 20 (2), 173–185.
Young, T.J., Cui, Y., Pfeffer, C., Hobbs, E., Liu, W., Irudayaraj, J., et al., 2020. CAF-1 and Rtt101p function within the replication-coupled chromatin assembly network to promote H4 K16ac, preventing ectopic silencing. PLoS Genet. 16, 1–35.
Yuan, Z.-F., Sidoli, S., Marchione, D.M., Simithy, J., Janssen, K.A., Szurgot, M.R., et al., 2018. EpiProfile 2.0: a computational platform for processing epi-proteomics mass spectrometry data. J. Proteome Res. 17 (7), 2533–2541.

Zhang, X., Noberini, R., Bonaldi, T., Seidl, M.F., 2021. Histone extraction for mass spectrometry-based analysis of post-translational modifications in the fungal genus *Aspergillus*. 2021. dx.doi.org/1017504/protocols.io.btpinmke.

Zhang, Y., Fan, J., Ye, J., Lu, L., 2021. The fungal-specific histone acetyltransferase Rtt109 regulates development, DNA damage response, and virulence in *Aspergillus fumigatus*. Mol. Microbiol. 115 (6), 1191–1206.

Zhang, X., Noberini, R., Bonaldi, T., Collemare, J., Seidl, M.F., 2022. The histone code of the fungal genus *Aspergillus* uncovered by evolutionary and proteomic analyses. Microb. Genom. 8.

Zhou, M., Malhan, N., Ahkami, A.H., Engbrecht, K., Myers, G., Dahlberg, J., et al., 2020. Top-down mass spectrometry of histone modifications in sorghum reveals potential epigenetic markers for drought acclimation. Methods 184 (October 2019), 29–39.

Zhuang, Z., Pan, X., Zhang, M., Liu, Y., Huang, C., Li, Y., et al., 2022. Set2 family regulates mycotoxin metabolism and virulence via H3K36 methylation in pathogenic fungus *Aspergillus flavus*. Virulence 13 (1), 1358–1378.